Acta Cryst. (1984). B40, 169–179

Diffraction Study of the Electron Density Distribution in Beryllium Metal

BY FINN KREBS LARSEN

Department of Inorganic Chemistry, Aarhus University, DK-8000 Aarhus C, Denmark

AND NIELS KRISTIAN HANSEN*

Hahn-Meitner-Institut für Kernforschung, Glienicker Strasse 100, D-1000 Berlin 39, Federal Republic of Germany

(*Received* 19 *January* 1983; *accepted* 21 *September* 1983)

Abstract

Deformation and valence density maps for beryllium metal are calculated by Fourier summations of X-ray structure factors derived from a full sphere of Mo $K\alpha$ and a half sphere of Ag $K\alpha$ diffraction data. Scale factor and extinction parameters of the X-ray structure factors are judged by comparison with γ-ray structure factors. Mean-square amplitudes determined from high-order refinement of the X-ray data [$u_{11} = 0.00619\,(2)$, $u_{33} = 0.00543\,(3)$ Å^2] are slightly higher than values previously determined in a short-wavelength neutron diffraction study [$u_{11} = 0.00597(3)$, $u_{33} = 0.00540(3)$ Å^2]. The high-order refinement using a free-atom scattering factor shows that the core electron distribution conforms very closely with a free-atom description [$R(F^2) = 0.005$]. Deformation ($X - X_{\text{high}}$, $X - N$ and $X - \gamma - N$) and valence density maps show surplus of charge in the tetrahedral holes of the hexagonal-close-packed structure and charge deficiency in the channels formed by adjoining octahedral holes. Charge integration over the bipyramidal space of two adjacent tetrahedral holes amounts to 0.013(2) electrons. Experimental diffraction results are in very good agreement with recent *ab initio* calculations, as well with an HF–SCF–LCAO as with a pseudopotential calculation while APW calculations appear to exaggerate the p_z contribution to the crystal wave function. High-order refinement using a scattering factor derived from the LCAO calculation leads to temperature factors [$u_{11} = 0.00605(1)$, $u_{33} = 0.00528\,(2)$ Å^2] that agree well with the neutron values which may indicate a slight core expansion. {Crystal data: space group $P6_3/mmc$, $a = 2.2853(3)$, $c = 3.5842(2)$ Å, $V = 16.218$ Å^3, $Z = 2$, $D_x = 1.845$ g cm^{-3}, μ(Mo $K\alpha$) = 0.55 cm^{-1}. Values of Mackay & Hill [*J. Nucl. Mater.* (1963). **8**, 263–267]: $a = 2.2858(2)$, $c = 3.5843(3)$ Å.}

Introduction

The charge density distribution in beryllium has been the subject of a number of diffraction studies. Brown (1972) measured structure factors with Ag $K\alpha$ X-radiation in order to establish and analyze the experimental atomic scattering factor. Brown noted that beryllium is a particularly suitable material in which to look for effects in the electron distribution caused by interatomic binding in the crystal because two of the four electrons of each beryllium atom are valence electrons which may be supposed to play a part in bonding. Brown published the 27 lowest-angle structure factors deduced on absolute scale from integrated intensities of Bragg reflections from two single-crystal plates measured in equatorial transmission geometry. Analysis of the data provided evidence that the valence electrons in beryllium metal are *p*-like in character with p_z-type wave functions accounting for rather more than one third of the occupied states. Brown's X-ray structure factors were used in further analyses of the electron density distribution by Stewart (1977) and Yang & Coppens (1978).

Stewart applied a rigid pseudoatom model, fitting by a least-squares technique an atom-centered valence monopole plus three higher multipoles to the experimental data. The superposition of these density functions gave valence maps showing bonding charge density between beryllium atoms along the *c* axis through the tetrahedral hole of the hexagonal-close-packed structure. Yang & Coppens in their study calculated valence and deformation density maps by direct Fourier transformation of the experimental structure factors using thermal parameters determined by least-squares refinements of reflections with $\sin\theta/\lambda \geq 0.5$ Å^{-1}. They interpreted their maps to indicate covalent bonding which they expressed in terms of a hybrid orbital model as $(sp^2)^a(sp)^b$. The density maps showed that the *sp* hybrids taken to point in the direction of the *c* axis have more density than the sp^2 orbitals located in the basal plane and therefore $b > a$. Yang & Coppens noted that this is in full agreement with the observation that the axial

* Present address: Laboratorie de Minéralogie et Cristallographie, Université de Nancy I, BP 239, F-54506 Vandoeuvre-Les-Nancy CEDEX, France.

0108-7681/84/030169-11$01.50

ratio $c/a = 1.568$ is smaller than the value of 1.633 for an ideal hexagonal-close-packed structure.

Inoue & Yamashita (1973) performed an augmented plane wave (APW) calculation and published a theoretical valence density map. The position and peak height of the local maximum near the tetrahedral hole in this map agree remarkably well with the experimental maps [Inoue & Yamashita (1973): 0.32 eÅ^{-3}; Yang & Coppens (1978): 0.37 (2) eÅ^{-3}, Stewart (1977): 0.33 eÅ^{-3}]. It should be remarked that this local maximum near the tetrahedral hole is not very pronounced. Features in the valence map are superimposed on an average background level of 0.247 eÅ^{-3} from the valence electrons. The most prominent feature in the valence map was a strongly negative area around the atomic position which may, however, not be statistically significant because errors in the experimental maps accumulate at atomic positions. The electron-deficient areas at or near the atomic cores could, however, be an indication of core polarization or anharmonic thermal motion of the nucleus.

Larsen, Lehmann & Merisalo (1980) determined from short-wavelength neutron data the mean-square atomic displacement and antisymmetric vibrations in beryllium and established that the vibrational anharmonicity is too insignificant to be the cause of the high-angle residuals shown by Stewart (1977) in refinements of Brown's (1972) structure factors. The neutron study gave values for the mean-square amplitudes [$u_{11} = 0.00597$ (3), $u_{33} = 0.00540$ (3) Å^2] significantly and strikingly smaller than values which Yang & Coppens (1978) derived from Brown's (1972) X-ray data [$u_{11} = 0.00759$ (12), $u_{33} = 0.00686$ (10) Å^2]. A straightforward explanation for such a discrepancy would be that core electrons in the metallic form of beryllium are significantly expanded relative to those of the free atom. Incidentally, this observation supports the similar conclusion by Weiss (1978) who calculated the cohesion energy of beryllium from experimental X-ray Compton profile data and found the result to be at variance with the experimentally determined value which he attributed to a shift of the momentum distribution in the solid from high to low momenta consistent with a core expansion. The discrepancies between neutron and X-ray values for the mean-square amplitudes of thermal vibration were, however, so substantial that the X-ray structure factors were remeasured by Manninen & Suortti (1979). Also, the Compton profile measurements were done anew (Manninen & Suortti, 1979; Hansen, Pattison & Schneider, 1979). Manninen & Suortti's X-ray diffraction study was performed on a single-crystal wafer in the symmetrical Laue geometry in much the same way as Brown's (1972) study, though they measured each single reflection on absolute scale. Intensities of high-order $h0l$ reflections only were measured, but the measurements were extended to larger scattering vectors ($0.74 < \sin\theta/\lambda < 1.40$ Å^{-1}) than in Brown's study ($\sin\theta/\lambda < 0.88$ Å^{-1}). Manninen & Suortti obtained thermal parameters $u_{11} = 0.00583$ (13), $u_{33} = 0.00526$ (13) Å^2, which are not significantly different from the neutron values. The Compton profile measurements agreed completely with the free-atom values for momentum values above $p \geq 2$ a.u. which substantiated the conclusion of the diffraction experiment, namely that the free-atom calculation gives an adequate description of the 1 *s* core in solid beryllium.

Suortti (1982) furthermore has reported the three lowest-order reflections for beryllium measured on an absolute scale using molybdenum and copper $K\alpha$ radiation. By comparing the measured reflections for different wavelengths and for different polarization of the incident beam, the integrated intensities measured from an extended plate were corrected for effects of both secondary and primary extinction.

The doubt cast on Brown's (1972) X-ray structure factors because of the discrepancies between X-ray and neutron values for the mean-square amplitudes also prompted the present reinvestigation of the charge density distribution in beryllium through new measurements of a complete set of X-ray structure factors. The valence-electron distribution must be very diffuse and will mainly contribute to the very-lowest-angle reflections. Unfortunately, these low-order reflections very often suffer from extinction so a γ-diffraction study (Hansen, Schneider & Larsen, 1983) of the innermost reflections was also carried out to provide an independent set of structure factors for comparison. The γ-ray diffraction data are measured on an absolute scale and are essentially free from extinction due to the very short wavelength of 0.03 Å of the 412 keV γ-radiation from the radioactive gold source.

Recently, another theoretical calculation on metallic beryllium appeared in the literature (Dovesi, Pisani, Ricca & Roetti, 1982). It is an *ab initio* Hartree–Fock (HF) self-consistent-field (SCF) linear-combination-of-atomic-orbitals (LCAO) calculation using an extended Gaussian basis set. This study, like the APW study by Inoue & Yamashita (1973), indicates that *p*-type functions play an important role in the bonding in beryllium metal. A new theoretical study of beryllium with APW technique (Redinger, Bauer & Hansen, 1984) produced a valence map almost identical to that of Inoue & Yamishita. Valence maps based on the two types of theoretical calculations nevertheless deviate in essential features which can be traced back to significant difference between the $F(002)$ structure-factor calculation on the basis of the two theories. Chou, Lam & Cohen (1983) have calculated charge densities and structure factors from wave functions obtained from a pseudo-potential band-structure calculation using a non-local pseudopotential and treating electron–electron correlation within

the local density approximation. The relative success of the different theories in describing valence and deformation electron densities in beryllium is discussed in the conclusion.

Experimental

From an experimental diffraction point of view, beryllium offers the advantage of a very high Debye temperature which means that mean-square amplitudes even at room temperature of 295 K are so small that beryllium diffracts well out to very high values of $\sin\theta/\lambda$. The experimentally simpler and more accurate room-temperature study in this sense efficiently equals a low-temperature study. The excellent diffraction properties also allow use of a very small sample crystal which secures a good homogeneity of the part of the X-ray beam hitting the crystal. As a further benefit of a small sample crystal, extinction will be minimal.

A fragment of the same ten-pass zone-refined crystal which yielded the crystal used in the neutron diffraction studies of the thermal vibrations in Be (Larsen *et al.*, 1980; Larsen, Brown, Lehmann & Merisalo, 1982) was arc cut and subsequently etched to the dimensions $0.1\times0.25\times0.30$ mm with limiting planes of best simple indexing $(2\bar{1}0)$, (100) and (001). The crystal was mounted in an arbitrary orientation on a Picker FACS-1 automatic diffractometer. Unit-cell dimensions were obtained by least-squares refinement of the observed setting angles for the $K\alpha_1$ peaks of 14 centered reflections with $2\theta>60°$. Crystal data for Be are summarized in the Abstract.

Intensity measurements were collected with Zr-filtered Mo $K\alpha$ and with Pd-filtered Ag $K\alpha$ radiation using ω–2θ step scans. Reflections were scanned from $2\theta(K\alpha_1)-1.90°$ to $2\theta(K\alpha_2)+1.90°$ in steps of 0.04° in 2θ and with a counting time of 4 s per step. Observed step counts were corrected for coincidence loss and correction for Lorentz–polarization effects was applied.

Integrated intensities were evaluated by the minimal $\sigma(I)/I$ criteria (Lehmann & Larsen, 1974). In the experiment using Mo radiation, the full sphere of data out to $2\theta=120°$ ($\sin\theta/\lambda\le1.219$ Å^{-1}) was collected. It can be noted that the FWHM of some reflections vary considerably within some forms (*e.g.* between 0.28 and 1.04° for {011}), whereas the integrated intensities do not differ significantly (the difference between maximal and minimal observed intensity for {011} is 2.5%). This is believed to indicate that extinction for this small sample crystal is minute. Three standard reflections measured after every 25 reflections showed no significant trend in intensity during data collection. For each reflection the mean path length was calculated and in spite of the small magnitude of the absorption coefficient intensities were corrected for absorption (correction factors range from 0.990 to 0.995). The method used was Gaussian numerical integration (Coppens, Leiserowitz & Rabinovich, 1965). Symmetry-related reflections among the 1091 measurements with Mo $K\alpha$ radiation were averaged to give a final set of 74 independent reflections with internal agreement factors of $R_I(F^2)=0.008$ and $wR_I(F^2)=0.014$ [$R_I(F^2)=\sum|F^2-\langle F^2\rangle|/\sum F^2$ and $wR_I(F^2)=\sum|F^2/\sigma F^2-\langle F^2/\sigma F^2\rangle|/\sum F^2/\sigma F^2$].

In the experiment using Ag radiation half a sphere of data out to $2\theta=110°$ ($\sin\theta/\lambda\le1.46$ Å^{-1}) was collected. The counting time per step was the same as in the experiment with Mo radiation which means that the counting statistical errors in the intensities are relatively bigger in the Ag radiation experiment. Symmetry-related reflections among the 938 measurements were averaged to give a final set of 119 independent reflections with internal agreement factors $R_I(F^2)=0.020$ and $wR_I(F^2)=0.024$. The relatively bigger counting statistical error and the increased number of weak high-order reflections account for the agreement factors of the Ag radiation experiment being inferior to those of the Mo radiation experiment.

The measured intensities were corrected for thermal diffuse scattering (TDS) by using a program (Merisalo & Kurittu, 1978) which takes into account the anisotropic nature of the TDS. Elastic constants are given by Smith & Arbogast (1960). The magnitude of the TDS correction corresponds to an increase of the mean-square amplitude of vibration of 0.00010 Å^2 over the value which would be determined from integrated intensities uncorrected for TDS. Corrections to intensities amount to less than 0.1% for low-order reflections with $\sin\theta/\lambda<0.3$ Å^{-1} and less than 0.25% for $0.3<\sin\theta/\lambda<0.5$ Å^{-1}. The maximum TDS correction factor for the Mo data is 2.6% and for the Ag data 5.5%.

The X-ray data were corrected for an estimated average multiple scattering effect (Le Page & Gabe, 1979). The Mo data included 14 and the Ag data 20 measured space-group absences. In by far the most cases they were observed positive, although very small ($\le1\sigma$). The predicted [Fig. 5(*i*), Le Page & Gabe, 1979] diminishing tendency as a function of $\sin\theta/\lambda$ of the intensity from multiple scattering could not be established. Instead an average contribution was deduced and subtracted from all intensities. The average values for the Mo data amount to 0.002% of the intensity of the strongest reflection, $F^2_{\rm Mo}(002)$, and for the Ag data similarly to 0.02% of $F^2_{\rm Ag}(002)$. The neutron results of Larsen *et al.* (1980) originally were not corrected for multiple scattering. A reinvestigation of the neutron data revealed that the short-wavelength data were also influenced by multiple scattering as judged from the significant intensities of the absolute space-group-forbidden reflections. The average value amounts to 0.1% of the intensity

of the strong reflection, $F^2(002)$. Correction for this effect in the neutron case increases the mean-square amplitudes by one standard deviation, 0.00003 Å^2, relative to the values published by Larsen *et al.* (1980).

Analysis of data

The thermal motion in beryllium is nearly isotropic; therefore a good estimate of the general quality of the data and especially of the relative importance of extinction in the low-order data can be obtained from a Wilson plot. The crystal structure of beryllium at room temperature is hexagonal close packed with two atoms in the unit cell in positions of point symmetry $\bar{6}m2$ with coordinates $\pm(1/3, 2/3, 1/4)$. The structure factor takes the form

$$F_c(hkl) = 2f_{Be}(hkl)\cos 2\pi[(h+2k)/3 + l/4]T(hkl)$$
$$= f_{Be}(hkl)C(hkl)T(hkl).$$

The trigonometric factor $C(hkl)$ has one of four values 0, 1, $\sqrt{3}$, 2, thus giving three groups of non-zero reflections. The atomic scattering factor, $f_{Be}(hkl)$, was taken from *International Tables for X-ray Crystallography* (1974). Under the assumption of isotropic thermal movement the temperature factor $T(hkl)$ can be written

$$T(hkl) = \exp\{-8\pi^2\langle u^2\rangle[\sin\theta(hkl)/\lambda]^2\}$$

and with $F_o(hkl) = kF_c(hkl)$ the Wilson (1942) plot takes the form

$$\ln[F_o(hkl)/f_{Be}(hkl)C(hkl)]$$
$$= \ln k - 8\pi^2\langle u^2\rangle \sin^2\theta(hkl)/\lambda^2.$$

Fig. 1 shows the Wilson plot of the Mo $K\alpha$ and the Ag $K\alpha$ data. Neither the Ag $K\alpha$ nor the Mo $K\alpha$ low-order data show noticeable systematic deflection below the '00l' and 'hk0' lines which they would had the data been influenced much by extinction. The primary conclusion from inspection of Wilson plots of the data sets collected with the two different wavelengths is that the present beryllium sample seems to give insignificant extinction.

In the harmonic approximation just four parameters suffice for describing the structure, namely a scale factor, an isotropic secondary-extinction parameter, and the two thermal parameters u_{11} and u_{22}, that is the mean-square amplitudes of motion in the basal plane, $\langle u_x^2\rangle$, and along the 6_3 axis of the hexagonal-close-packed structure, $\langle u_z^2\rangle$.

The quantity $\sum w(F_o^2 - k^2F_c^2)^2$ with $w = 1/\sigma^2(F^2)$ was minimized by full-matrix least-squares refinement.

For both Mo and Ag data there is very close correspondence between the variance based on counting statistics, σ_c^2, and the sample variance, σ_s^2, calculated as $\sigma_s^2 = \sum^n (F_i^2 - \langle F^2\rangle)^2/(n-1)$, where n refers to the number of symmetry-related reflections. The estimated variance, $\sigma^2(F^2)$, used in the weighting was taken as the larger of the two, with an additional contribution proportional to F^2 according to the expression

$$\sigma^2(F^2) = \max(\sigma_c^2, \sigma_s^2) + p^2F^4.$$

In order to achieve even weighting over the total data set a value of $p = 0.025$ must be assigned to low-order reflections, while $p = 0.005$ for reflections with $\sin\theta/\lambda \geq 0.65$ Å^{-1}. Table 1 shows results of different refinements and structure-factor calculations. It may be noted that mean-square amplitudes refined from the two sets of data, Mo $K\alpha$ and Ag $K\alpha$, are not significantly different; however, their values are bigger than the values determined in the neutron diffraction study.

An isotropic type I extinction model with a Lorentzian mosaic distribution (Becker & Coppens, 1974) was applied to refinements of the complete Mo $K\alpha$ and Ag $K\alpha$ data sets. Scale factor and u's were kept at the values determined in the high-order refinements. Values of the secondary extinction parameters became for the Ag data $g_{Ag} = 0.006$ (46) (which corresponds to maximum correction of $<1\%$), and for the Mo data $g = -0.06$ (3). The finding that extinction for this tiny beryllium sample is vanishingly small is in accordance with expectations from the study of the Wilson plots. The value $g_{Ag} = 0.006$ was used throughout refinement for both data sets.

Implications of scale factor and thermal parameters

The scale factors for both Mo and Ag radiation data were established from high-order refinements. This

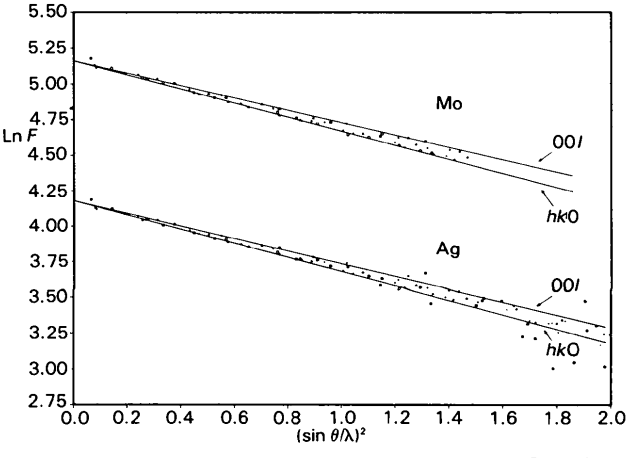

Fig. 1. Wilson plot, $\ln[F_o(hkl)/f_{Be}(hkl) \times C(hkl)] = \ln k - 8\pi^2\langle u^2\rangle[\sin\theta(hkl)/\lambda]^2$ of the Mo $K\alpha$ and Ag $K\alpha$ X-ray data. The three groups of non-zero reflections are entered with separate marks. △ for the strongest, *i.e.* $C(hkl) = 2$, + for $C(hkl) = \sqrt{3}$, and □ for the weakest, *i.e.* $C(hkl) = 1$. The '00l' line drawn through 00l reflections has smaller slope than the 'hk0' line drawn through hk0 reflections, indicating $\langle u_x^2\rangle > \langle u_z^2\rangle$.

Table 1. *Results of refinements (R) and structure-factor calculations (C)*

Expressions for agreement factors and goodness-of-fit are $R(F^2)=\sum|F^2_{obs}-F^2_{calc}|/\sum F^2_{obs}$; $wR(F^2)=[\sum w(F^2_{obs}-F^2_{calc})^2/\sum wF^4_{obs}]^{1/2}$; $GOF=[\sum w(F^2_{obs}-F^2_{calc})^2/(N_{obs}-N_{var})]^{1/2}$.

	$\langle\sin\theta/\lambda\rangle$ (Å^{-1})	N_{obs}	Scale	$\langle u_x^2\rangle$ (Å^2)	$\langle u_z^2\rangle$ (Å^2)	$R(F^2)$	$wR(F^2)$	GOF
Mo $K\alpha$	0.65, 1.21	46 *R*	173.9 (3)	0.00620 (3)	0.00543 (3)	0.004	0.007	0.99
Mo $K\alpha$	0, 1.21	58 *C*	173.9	0.00620	0.00543	0.015	0.019	1.04
Ag $K\alpha$	0.65, 1.41	71 *R*	64.8 (2)	0.00616 (4)	0.00544 (5)	0.012	0.015	0.99
Ag $K\alpha$	0, 1.41	83 *C*	64.8	0.00616	0.00544	0.017	0.017	1.03
Ag $K\alpha$	0.65, 1.21	46 *R*	64.7 (2)	0.00615 (5)	0.00541 (6)	0.009	0.013	1.10
Ag $K\alpha$	0, 1.21	58 *C*	64.7	0.00615	0.00541	0.017	0.018	1.07
Joint AgMo	0.65, 1.21	92 *R*	64.8 (1), 173.8 (3)	0.00619 (2)	0.00543 (3)	0.005	0.009	1.04
Joint Ag Mo	0, 1.21	116 *C*	64.8, 173.8	0.00619	0.00543	0.016	0.011	1.07
Averaged Ag Mo	0, 1.21	58 *C*	1.000	0.00619	0.00543	0.013	0.008	1.16
Averaged Ag Mo, Dovesi f_{Be}	0.65, 1.21	46 *C*	1.007	0.00605 (1)	0.00528 (2)	0.006	0.008	1.35
Averaged Ag Mo, Dovesi f_{Be}	0, 1.21	58 *C*	1.007	0.00605	0.00528	0.017	0.010	1.37
Neutron (Larsen *et al.*, 1980)		*R*		0.00597 (3)	0.00540 (3)			
$X-N$	0.65, 1.21	46 *R*	0.990 (1)	0.00597	0.00540	0.009	0.013	2.03
$X-N$	0, 1.21	58 *C*	0.990	0.00597	0.00540	0.021	0.015	2.07
$X-\gamma-N$	0, 1.21	58 *C*	1.007	0.00597	0.00540	0.022	0.036	5.12
$X-\gamma-N$, Dovesi f_{Be}	0, 1.21	58 *C*	1.007	0.00597	0.00540	0.018	0.013	1.87

procedure has been shown to give scale factors accurate to better than 1% (Stevens & Coppens, 1975). Comparison of Mo and Ag data clearly showed the inferiority of the Ag high-order data. They do give mean-square amplitudes in good agreement with the Mo results but counting statistics are rather poor for the Ag high-order data, so it was decided to disregard for calculation of Fourier maps the Ag data with $\sin\theta/\lambda > 1.21$ Å^{-1}, which is the limit of the Mo data. Mo and Ag data were brought on a common scale by a high-order refinement of the combined data using as parameters separate scale factors but common thermal parameters. Results are found in Table 1 under the heading 'Joint AgMo'. The Mo and Ag data scaled in this manner were averaged (internal agreement 0.006) to a final set of X-ray structure factors on an absolute scale which are the basis of Fourier maps shown in later sections. The agreement factor for the averaged data using free-atom form factor and with values for mean-square amplitudes taken from the high-order refinement of the joint data sets is $R(F^2)=0.013$ for the 58 structure factors with $\sin\theta/\lambda \le 1.21$ Å^{-1}.

The absolute-scale γ-ray structure factors are on average a trifling 0.7% lower than the present X-ray data. This small difference, however, fits with the simple picture of a metal having valence electrons delocalized to an extent that the scattering power of the metal is less than that of a free atom, even for very high values of $\sin\theta/\lambda$. Scale-factor values which result from high-order refinements with higher cut-off values than the usual $\sin\theta/\lambda = 0.65$ Å^{-1} hint at the same explanation. The following sets of values for $\sin\theta/\lambda$, Ag scale factor, Mo scale factor were obtained; 0.65 Å^{-1}, 64.9 (1), 174.0 (4); 0.85 Å^{-1}, 65.2 (3), 174.5 (7); 1.00 Å^{-1}, 65.3 (6), 175.1 (1.6). It is questionable whether the scale factor of diffraction data from a light metallic substance can be determined very reliably by high-order refinement even using data of very high $\sin\theta/\lambda$ cut-off values.

The X-ray-determined mean-square amplitudes, in spite of careful data correction, appear to be bigger than the neutron values, u_{11} apparently significantly bigger. Several cases of systematic differences between X-ray and neutron thermal parameters are reported in the literature (see, for example, Coppens, Boehme, Price & Stevens, 1981). Frequently, the discrepancies are postulated to be due to differences either in data collection temperature or in background correction used in the two sets of measurements. In the case of beryllium, temperature ambiguity is ruled out since both neutron and X-ray data were collected at ambient temperature. Furthermore, a similar background correction technique, the $\sigma(I)/I$ method (Lehmann & Larsen, 1974), is applied and careful correction for TDS has been carried out for both neutron and X-ray data.

The explanation for the observation that X-ray thermal parameters are bigger than the neutron values might be that the metallic beryllium core electrons have expanded relative to the free-atom core.

An actual core expansion will influence not only the thermal parameters but also the scale factor when determined from a high-order refinement. Intensity will have shifted towards lower $\sin\theta/\lambda$ values and consequently the scale factor determined from a high-order refinement of X-ray data will tend to become too small (scale factor divides F_{obs}). This explanation also conforms with the observation that the absolute γ-ray intensities appear to be an average 0.7% lower

than the X-ray intensities. An experimental atomic form factor can be deduced from the X-ray data by allowing the thermal parameters to have the neutron values and including a scale factor which brings the X-ray structure factors on the level of the γ-ray structure factors. The deviation of such an experimental atomic scattering factor, f_{exp}, from the free-atom form factor is depicted in Fig. 2 which shows ($|f_{exp}| - |f_{free\ atom}|$) as a function of sin θ/λ. The f_{exp} values are calculated from the structure factors by correcting for the trigonometric factor and the temperature factor. The deviation at higher values of sin θ/λ could be explained as due to a core expansion and the effect is thus quite small, on the limit of being significant as deduced from the present data. $\Delta u_{ii} = u_{ii}$ (X-ray) $- u_{ii}$ (neutron) is significantly bigger for $i = 1$ than for $i = 3$, which might imply anisotropic core expansion. The expansion appears to be the bigger in the basal plane of the h.c.p. lattice.

Dovesi, Angonoa & Causa (1983) concluded from their *ab initio* HF–SCF–LCAO calculation that 'the expansion of the beryllium core in the metal with respect to the isolated atom appears to be a minor effect, though not a negligible one'. They calculated the differences between structure factors for the metal and the isolated-atom case. Core contributions deviate less than 0.5% while the total differences are in the range 1.4–2.0% for higher sin θ/λ values, which is quite similar to the comparable experimental differences shown in Fig. 2. Although the theoretical calculation indicates the core expansion to be slightly anisotropic, consistent with the experimental observation, we have deduced from the theoretical calculation an average experimental atomic form factor for metallic beryllium and used it in a high-order refinement of the thermal parameters using the averaged structure factors scaled to the level of the γ data.

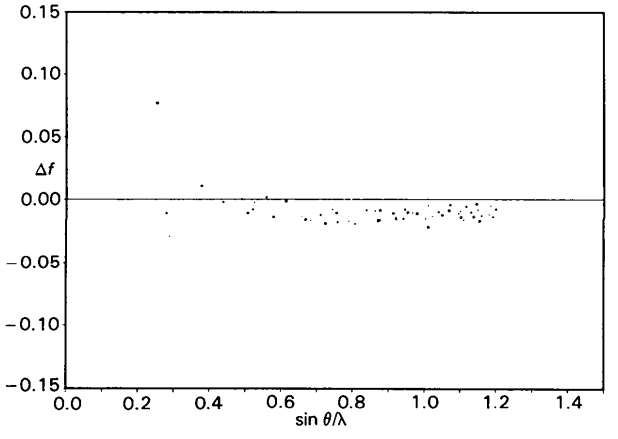

Fig. 2. Deviation of the experimental atomic scattering factors from the free-atom Hartree–Fock form factor. X-ray structure factors were scaled to the level of the γ-ray structure factors and corrected for thermal vibration according to neutron thermal parameters. The average standard deviation is ~0.01 electrons.

Table 1 shows that the fit in this refinement (heading: 'Averaged AgMo, Dovesi f_{Be}') is comparable in quality with that using the free-atom form factor. Thermal parameters resulting from the latter refinement are hardly significantly different from the neutron values.*

Density mapping

Commonly used presentations of electron density distributions are deformation and valence density maps which are calculated according to the following Fourier summations:

$$\rho_{deformation}(\mathbf{r}) = \frac{1}{V}\sum_{\mathbf{H}} (F_{obs}k^{-1} - F_{free\ atom}) \times \exp(-2\pi i \mathbf{H}\,.\,\mathbf{r})$$

$$\rho_{valence}(\mathbf{r}) = \frac{1}{V}\sum_{\mathbf{H}} (F_{obs}k^{-1} - F_{core}) \exp(-2\pi i \mathbf{H}\,.\,\mathbf{r}).$$

F_{obs} are the observed structure factors and k is the scale factor. $F_{free\ atom}$ are the theoretical structure factors corresponding to the free-atom model and corrected for the thermal motion. $F_{free\ atom}$ are calculated using the relativistic HF scattering factor (*International Tables for X-ray Crystallography*, 1974). A scattering factor calculated from a multiconfiguration wave function (Sabin, 1983), and thus taking correlation into consideration, was also tested as a reference free-atom state. The maximum deviation between the RHF and the MC–SCF form factors is 1.3% at sin $\theta/\lambda \simeq 0.15$ Å^{-1}. However, for the lowest-order reflection in beryllium metal at sin $\theta/\lambda = 0.253$ Å^{-1} the difference is only 0.4% and it is less than 0.2% for the rest of the reflections. Deformation maps calculated with the two different scattering factors are very similar. F_{core}, which are the core-electron parts of the free-atom structure factors, are calculated using Fukamachi's (1971) scattering factor for beryllium. For scale factor and thermal parameters determined from high-order refinement of the X-ray data the corresponding representations of electron density distributions are termed $X - X_{high}$ maps while maps calculated with high-order scale and neutron thermal parameters are termed $X - N$ maps.

Fig. 3 is a drawing of the hexagonal-close-packed beryllium structure depicting 99.99% thermal ellipsoids. The shaded area within the outlined unit cell is the (110) plane which goes through nearest-neighbour atoms; for beryllium metal that is the atoms from adjacent basal planes of the stacking sequence *ABAB*....

* Lists of structure factors have been deposited with the British Library Lending Division as Supplementary Publication No. SUP 38852 (4 pp.). Copies may be obtained through The Executive Secretary, International Union of Crystallography, 5 Abbey Square, Chester CH1 2HU, England.

Deformation maps

The least-squares analysis showed that the experimental structure factors of beryllium metal are very similar to the theoretical structure factors calculated for a free-atom model.

The most informative way of illustrating the minute redistribution of electrons relative to the free-atom model is as deformation density maps. Fig. 4 shows the $X - X_{high}$ deformation density map of the (110) plane. Fig. 5 presents sections of the $X - X_{high}$ deformation map parallel to (001). Section 5(*a*) is the hexagonal close-packed basal plane, $Z = 0.75$, with atomic positions in the corners of the map. Section 5(*b*) has $Z = 0.625$ and so contains a tetrahedral site, and section 5(*c*) has $Z = 0.500$ and contains an octahedral site. Peaks and holes in the $X - X_{high}$ maps are low (less than ± 0.05 e Å^{-3}) and smooth. The most conspicuous features are the surplus of electrons in the bipyramidal space around the tetrahedral hole and the deficiency of electrons in the channel formed by the adjoining octahedral holes along the *c* axis through the h.c.p. structure. This redistribution of electrons does not imply a simple covalent bonding scheme. The difference density between nearest as well as next-nearest neighbor atoms is practically zero. Only the third-neighbor direction which goes through the tetrahedral holes has a peak, a double maximum of height 0.046 e Å^{-3}.

The $X - N$ map of the (110) plane, Fig. 6, differs only insignificantly from the $X - X_{high}$ map in the regions away from the atomic center. The differences between the maps in the core region are results of the smaller and more anisotropic thermal parameters obtained from the neutron diffraction analysis.

Difference structure factors from a structure-factor calculation with thermal parameters fixed at the neutron values and with the scale factor which brings the X-ray structure factors on to the level of the absolute γ-ray structure factors produce a deformation map which may be termed an $X - \gamma - N$ map and the (110) plane is shown in Fig. 7. The area around the nucleus becomes strongly negative (-0.45 e Å^{-3}), and the difference in anisotropy between high-order X-ray and neutron thermal parameters produces the sharp positive feature 0.4 Å

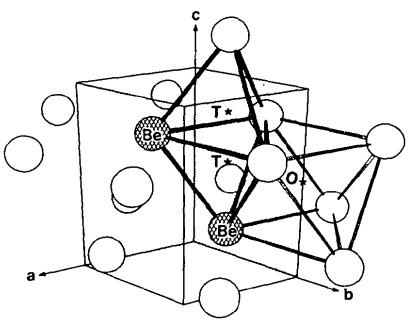

Fig. 3. The hexagonal-close-packed beryllium structure. The shaded area within the outlined unit cell is the (110) plane which goes through the centers of the tetrahedral holes, marked *T*, and through the centers of the octahedral holes, marked *O*.

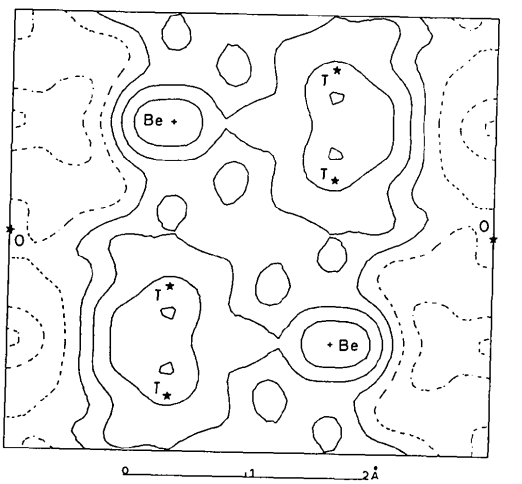

Fig. 4. $X - X_{high}$ deformation map in the (110) plane, with *z* direction vertical. The section displays the electron deficiency along the channels formed by adjoining octahedral holes, marked *O*, and the surplus of charge in the bipyramidal space around the tetrahedral holes, marked *T*. Contours are plotted at 0.015 e Å^{-3} intervals with negative contours as broken lines. The first solid line is the zero contour.

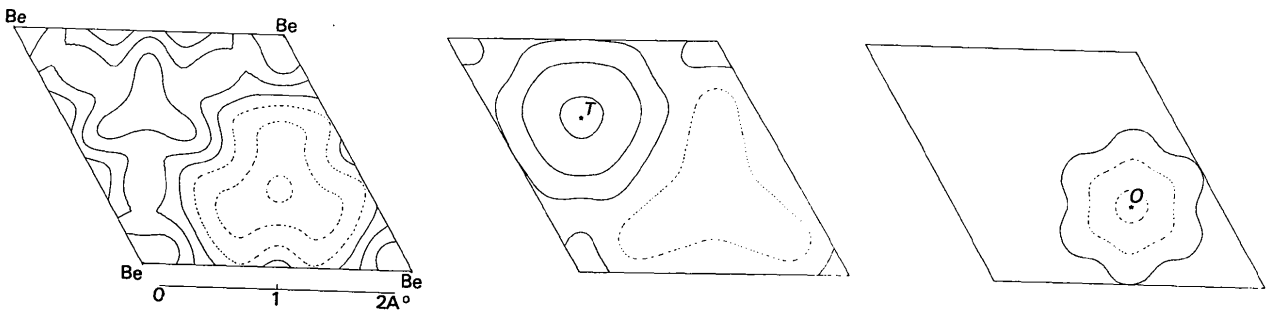

(*a*) (*b*) (*c*)

Fig. 5. $X - X_{high}$ deformation map in sections parallel to (001). Contours as in Fig. 4. Section (*a*) at $z = 0.75$ contains the atomic position, section (*b*) at $z = 0.625$ goes through the tetrahedral position (*T*), and section (*c*) at $z = 0.500$ through the octahedral position (*O*).

from the atomic position. The qualitative appearance of the different deformation maps, Figs. 4, 6 and 7, is quite similar outside the vicinity of the nuclei. The height of the peak near the tetrahedral holes is 0.046 e Å^{-3} for the $X - X_{high}$ and 0.040 e Å^{-3} for the $X - N$ map and 0.043 e Å^{-3} for the $X - \gamma - N$ map. A theoretical deformation density map (solid minus atomic superposition) for the LCAO calculation of Dovesi *et al.* (1983) is shown in Fig. 8. The theoretical structure factors calculated on the basis of the band-structure calculations were, before Fourier summation, corrected for the influence of thermal motion by applying the thermal parameters of the neutron diffraction study by Larsen *et al.* (1980). This theoretical map looks astonishingly like the $X - \gamma - N$ experimental map. The negative density near the nuclei was interpreted by Dovesi *et al.* to show the charge transfer from *s*-type functions to protruding *p*-type functions.

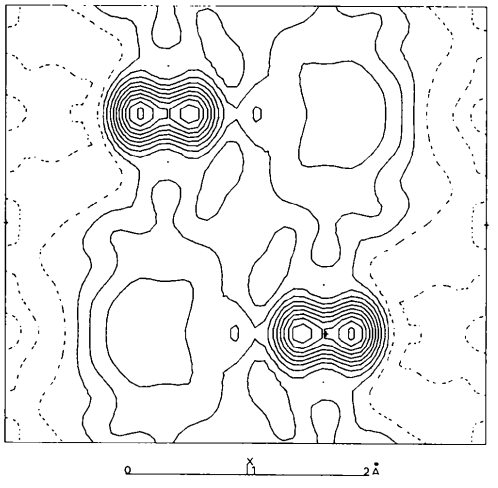

Fig. 6. $X - N$ deformation map in the (110) plane. Contours as in Fig. 4. The double peak around the atomic center is a result of the smaller and more anisotropic neutron thermal parameters.

Error map and charge integration

The significance of the features in the maps should be judged in the light of corresponding standard deviations. Error maps for the deformation density were calculated following Rees (1978). The error estimated for the scale is less than 0.2% according to the least-squares refinement of the high-order data and gives an estimate of the error at the atomic position of 0.035 e Å^{-3}, which is too optimistic. As seen in Table 1, scaling to the level of the γ-ray structure factors is associated with an increase in scale factor of 0.7% while the $X - N$ model refinement decreases the scale factor by 1.1%. In view of the different values obtained, a reasonable estimate seems to be a 1% error in the scale factor, which is, furthermore, the magnitude of error found by Stevens & Coppens (1975) in their study on scale factors. A 1% error in the scale factor makes the error in the deformation density at the nuclei peak at a value of 0.33 e Å^{-3}, while the values outside a radius of 0.4 Å from the nuclear position are very little changed relative to the errors calculated with the scale-factor error determined by least-squares refinement. The average error in the density calculated according to Cruickshank (1949) is 0.017 e Å^{-3}, and the detailed error map in the (110) plane calculated according to Rees (1978) is shown as Fig. 9. Errors are relatively high over the tetrahedral hole.

Values of the difference density at individual points in the deformation maps appear hardly significant, seemingly making any interpretation of features in the deformation maps quite hazardous. Nevertheless,

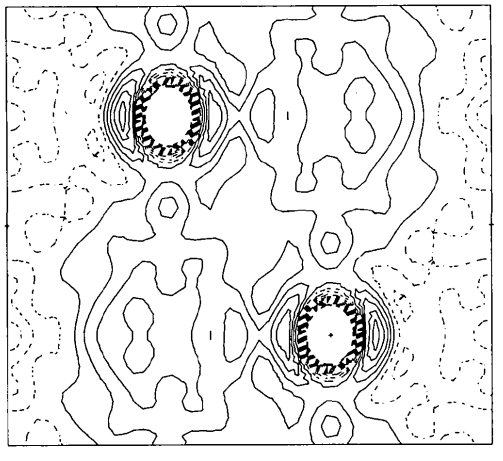

Fig. 7. $X - \gamma - N$ deformation map in the (110) plane. X-ray structure factors are scaled to the level of the absolute γ-ray structure factors and thermal parameters are fixed at the neutron values. Contours as in Fig. 4 with contours below −0.15 e Å^{-3} omitted.

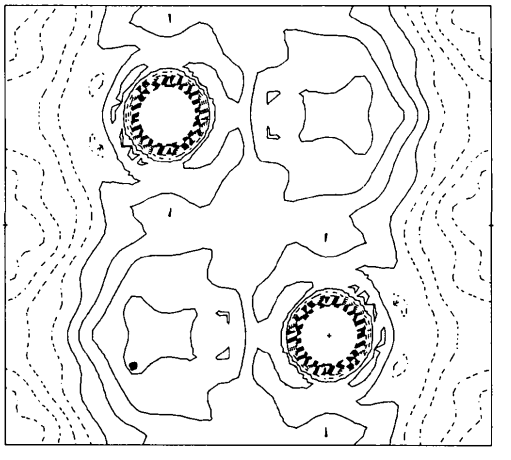

Fig. 8. Theoretical deformation map in the (110) plane. Density calculated from structure factors from LCAO band-structure calculation minus density of free atoms. Contours as in Fig. 7.

the deformation maps are very suggestive of a surplus of charge in the bipyramidal space of the structure, and this gross feature is significant. An integration of charge in the $X-\gamma-N$ deformation density distribution over an ellipsoidal volume (Coppens & Hamilton, 1968) with $R1=R2=0.7$ Å in the basal plane, and $R3=1.25$ Å along the c axis and centered on the midpoint between the tetrahedral holes gave an estimation of the charge in the bipyramidal space of 0.013 (2) electrons for the averaged Ag Mo data and 0.012 (1) electrons for the Mo data alone, a very small but significant charge redistribution relative to the free-atom model.

Valence maps

The electron distribution resulting from the theoretical APW calculation by Inoue & Yamashita (1973) was presented as a valence density map in the (110) plane. Stewart (1977) and Yang & Coppens (1978) showed similar valence maps calculated on the basis of their various treatments of Brown's (1972) X-ray data. For comparison, the $X-\gamma-N$ valence map of the present X-ray data is shown as Fig. 10. Yang & Coppens (1978) interpreted the density distribution as a bonding scheme of overlap of partially populated hybrid orbitals which were described as $(sp^2)^a(sp)^b$. The density distribution in their valence density maps is a little different from that of Fig. 10 due to the problems with Brown's data.

An alternative description to the one proposed by Yang & Coppens (1978) would be to assume sp^3 hybridization of the valence orbitals with one lobe, $\frac{1}{2}(s+3p_z)$, parallel to the c axis. The orientation should be identical for all atoms, and the other three lobes from one atom would be pointing into three of the tetrahedral holes around the atom. This means that each hybrid can be allocated $\frac{1}{2}$ of an electron and will be pointing towards the center of a tetrahedral cavity into which three other hybrids from the other atoms forming the cavity also will be pointing. Such four hybrid orbitals will only overlap strongly with each other and with no other orbital in this structure, and they might be thought of as forming a localized four-center two-electron bond. This bonding scheme takes care of the bonding through half of the tetrahedral holes, and is in agreement with the octet rule. By reflecting the hybrids (the atoms are lying on crystallographic mirror planes perpendicular to the c axis), *i.e.* the hybrid along the c axis takes the form $\frac{1}{2}(s-3p_z)$, we get the same configuration, but now filling the other half of the tetrahedral cavities. We may therefore describe the total bond structure as a resonance between these two bonding schemes. The idea conforms with the observation of a local maximum in the experimental valence density close to the center of the tetrahedral hole, and with the low values of the density in the octahedral holes.

The qualitative interpretation that bonding in beryllium is influenced by hybridization is supported by the recent calculation by Dovesi *et al.* (1983). Their band-structure and density-of-states calculations show that the role of p electrons in characterizing the ground state of beryllium is very important. Of the four valence electrons in the unit cell, 1.18 corresponds to s-type functions, 0.95 to p_x, 0.95 to p_y, and 0.92 to p_z atomic orbitals. Fig. 11 is the theoretical valence map corresponding to the calculation of Dovesi *et al.* It is noteworthy that the agreement with the $X-\gamma-N$ valence map, Fig. 10, is practically quantitative except near the center of the channel of octahedral holes. Inoue & Yamashita's (1973) APW

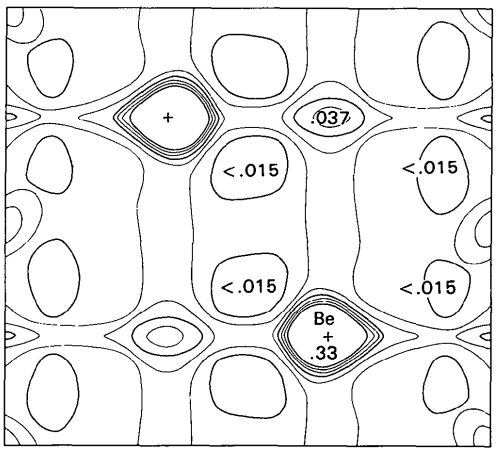

Fig. 9. Estimated error distribution of the deformation density in the (110) plane. Contours are plotted at 0.005 e Å^{-3} intervals starting at 0.015 e Å^{-3}. Contours at the intervals of 0.015 e Å^{-3} are drawn as a heavier line. Contours above 0.045 e Å^{-3} have been omitted.

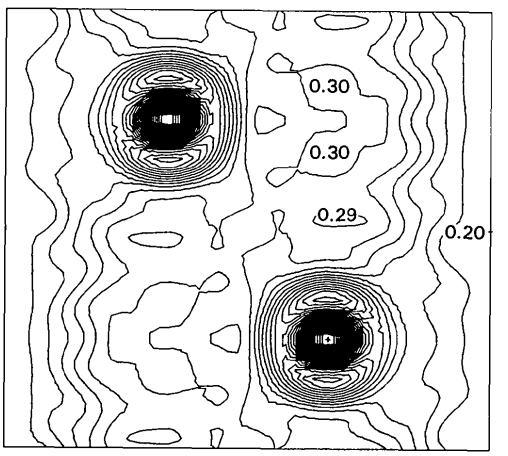

Fig. 10. $X-\gamma-N$ experimental valence map in the (110) plane. Contours are plotted at 0.015 e Å^{-3} intervals. The value at the atomic position is 0.49 e Å^{-3}. Units of numbers shown on the map are e Å^{-3}.

calculation gave a valence map which is somewhat at variance with Figs. 10 and 11 and is generally in poorer agreement with the present experimental valence map than the map from the LCAO calculation is.

Conclusion

The study of the electron density distribution in beryllium metal is based on 58 structure factors obtained by averaging experimental Mo $K\alpha$ and Ag $K\alpha$ X-ray diffraction data. The structure factors from the present study are on average 7% larger than those measured by Brown (1972). As discussed at some length by Hansen *et al.* (1983), Brown's data cannot be considered on an absolute scale and her low-order data are posssibly seriously affected by extinction. Therefore, electron densities calculated from her data are not reliable even though they are in agreement with the APW calculation by Inoue & Yamashita (1973). A high-order refinement ($\sin\theta/\lambda > 0.65$ Å^{-1}) using a free-atom form factor scales the experimental structure factors to values which are on average 0.7% higher than structure factors on an absolute scale measured by γ-radiation (Hansen *et al.*, 1983). This may indicate that the valence electrons are delocalized to an extent which makes the valence part of the metal form factor fall below that of the free atom far beyond a data cut-off of $\sin\theta/\lambda = 0.65$ Å^{-1}. The high-order refinement also resulted in higher values of the thermal parameters than obtained in a neutron diffraction study (Larsen *et al.*, 1980). This effect may indicate core expansion in beryllium metal which in the high-order refinement also will influence the scale factor and result in slightly high values of low-order structure factors. Whichever is the case, valence-electron delocalization or core-electron expansion, the conclusion must be that for a light-atom metallic substance a very reliable scale factor cannot be established from high-order refinement alone. Refinement using a form factor derived from the LCAO band structure calculation by Dovesi *et al.* (1982) with the X-ray data scaled to the absolute γ-ray data retrieved the neutron thermal parameters. This is taken to indicate that core expansion in beryllium metal is of the order of magnitude described in the theoretical calculation by Dovesi *et al.* (1983).

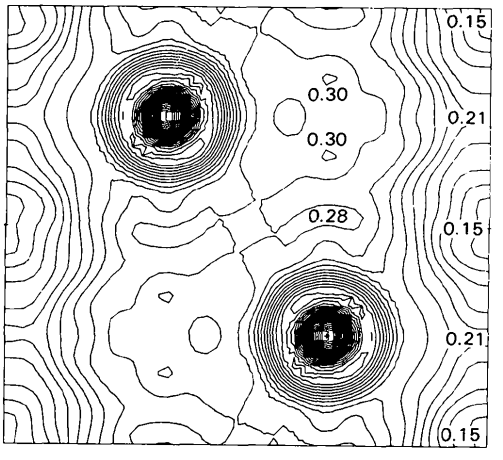

Fig. 11. LCAO theoretical valence map. Contours as in Fig. 10. The value at the atomic position is 0.44 e Å^{-3}. Units of numbers shown on the map are e Å^{-3}.

The bonding in beryllium metal was discussed on the basis of deformation and valence-electron density distributions; $X - X_{high}$ and $X - N$ maps were calculated. In the harmonic approximation the deformation density for beryllium metal only depends on scale factor and vibrational amplitudes as parameters. By scaling the X-ray structure factors to the level of the absolute γ-ray structure factors and using the neutron thermal parameters an electron density representation resting on no fitted parameters is obtained. We have termed maps of this type $X - \gamma - N$ maps. The different representations give very similar results outside a spherical volume of radius 0.4 Å around the atomic position. There is a surplus of electron density in the bipyramidal space around the pairs of adjoining tetrahedral holes in the h.c.p. structure which amounts to a charge of 0.013 (2) electrons, and there is a deficiency of electrons in the channels formed by the octahedral holes.

We note that theoretical calculations on clusters of beryllium atoms (Brewington, Bender & Schaefer, 1976) gave the result that tetrahedral Be_4 appears to be the smallest significantly bound beryllium metal cluster. Another Be_4 cluster calculation (Jordan & Simons, 1977) indicates that s and p atomic orbitals have hybridized such that charge density is localized in the interior of the tetrahedron, and in a calculation on small clusters of beryllium by Whiteside, Krishnan, Pople, Krogh-Jespersen, Schleyer & Wenke (1980) it was found that the trigonal bipyramidal pentamer was the most stable of Be_5 clusters but the binding per bond (41.0 kJ per bond) was smaller than for the tetragonal tetramer (47.2 kJ per bond) and still much smaller than the experimental heat of sublimation (53.9 kJ per bond).

The interpretation of the charge density distribution as derived from the present X-ray data can be based on a scheme of sp^3 hybridization. The bonding is imagined to be effected by a resonance between sp^3 orbitals directed towards the tetrahedral holes. In the h.c.p. structure two tetrahedral holes share a face and the resonance leads to a strong mixture of the four-center orbitals for two adjoining tetrahedra.

The experimentally determined maps of electron density distribution compare more favorably with results of LCAO (Dovesi *et al.*, 1983) than with APW (Redinger *et al.*, 1984) theoretical calculations.

The LCAO calculation gives a very satisfactory description of the charge distribution at almost all points, but does exaggerate slightly the depletion of charge in the octahedral holes when compared to experiment. In this latter region the APW calculation seems better while it is much less satisfactory around the tetrahedral-hole region. Recently, Chou, Lam & Cohen (1983) have made an *ab initio* self-consistent pseudopotential calculation of the structural and electronic properties of beryllium within the local density approximation. The valence charge density is a direct output of the pseudopotential crystal calculation, and it agrees with the $X-\gamma-N$ valence density within $\sim 1\sigma_{exp}$ at all points except near the nuclear position. With respect to the APW calculations, one can imagine two reasons why agreement with experiment is not perfect, namely the muffin-tin approximation and the local-density approximation used in the treatment of exchange and correlation. Since the pseudopotential calculation also employs the local-density approximation and is in very good agreement with experiment, we must take it that for the APW calculation on beryllium the muffin-tin approximation is too restrictive.

When it comes to comparison of theoretical total structure factors with the experimental values the pseudopotential calculation is inferior to the LCAO calculation. Chou, Lam & Cohen (1983) constructed total structure factors as the sum of the pseudo valence structure factor and the core structure factor from the HF band-structure calculation (Dovesi *et al.*, 1983). In the low-order region the agreement with experimental structure factors is good for the pseudopotential calculation, but in the high-order region the pseudopotential structure factors so obtained are significantly too weak. This may be due to the neglect of orthogonality corrections of the pseudo valence wave functions to the core orbitals.

Support of this work by the Danish Natural Science Research Council is gratefully acknowledged.

References

BECKER, P. J. & COPPENS, P. (1974). *Acta Cryst.* **A30**, 129–147.

BREWINGTON, R. B., BENDER, C. H. & SCHAEFER, H. F. (1976). *J. Chem. Phys.* **64**, 905–906.

BROWN, P. J. (1972). *Philos. Mag.* **26**, 1377–1394.

CHOU, M. Y., LAM, P. K. & COHEN, M. L. (1983). *Phys. Rev. B*, **28**, 4179–4185.

COPPENS, P., BOEHME, R., PRICE, P. F. & STEVENS, E. D. (1981). *Acta Cryst.* **A37**, 857–863.

COPPENS, P. & HAMILTON, W. C. (1968). *Acta Cryst.* **B24**, 925–929.

COPPENS, P., LEISEROWITZ, L. & RABINOVICH, D. (1965). *Acta Cryst.* **18**, 1035–1038.

CRUICKSHANK, D. W. J. (1949). *Acta Cryst.* **2**, 65.

DOVESI, R., ANGONOA, G. & CAUSA, M. (1983). Submitted to *Philos. Mag.*

DOVESI, R., PISANI, C., RICCA, F. & ROETTI, C. (1982). *Phys. Rev. B*, **25**, 3731–3739.

FUKAMACHI, T. (1971). *Tech. Rep. Inst. Solid State Phys., Univ. Tokyo, Ser. B*, No. 12.

HANSEN, N. K., PATTISON, P. & SCHNEIDER, J. R. (1979). *Z. Phys.* **B35**, 215–225.

HANSEN, N. K., SCHNEIDER, J. R. & LARSEN, F. K. (1983). *Phys. Rev. B.* In the press.

INOUE, S. T. & YAMASHITA, J. (1973). *J. Phys. Soc. Jpn*, **35**, 677–683.

International Tables for X-ray Crystallography (1974). Vol. IV. Birmingham: Kynoch Press.

JORDAN, K. D. & SIMONS, J. (1977). *J. Chem. Phys.* **67**, 4027–4037.

LARSEN, F. K., BROWN, P. J., LEHMANN, M. S. & MERISALO, M. (1982). *Philos. Mag.* **B45**, 31–50.

LARSEN, F. K., LEHMANN, M. S. & MERISALO, M. (1980). *Acta Cryst.* **A36**, 159–163.

LEHMANN, M. S. & LARSEN, F. K. (1974). *Acta Cryst.* **A30**, 580–584.

LE PAGE, Y. & GABE, E. J. (1979). *Acta Cryst.* **A35**, 73–78.

MACKAY, K. J. H. & HILL, N. A. (1963). *J. Nucl. Mater.* **8**, 263–267.

MANNINEN, S. & SUORTTI, P. (1979). *Philos. Mag.* **B40**, 199–207.

MERISALO, M. & KURITTU, J. (1978). *J. Appl. Cryst.* **11**, 179–183.

REDINGER, J., BAUER, G. & HANSEN, N. K. (1984). In preparation.

REES, B. (1978). *Acta Cryst.* **A34**, 254–256.

SABIN, J. R. (1983). Private communication.

SMITH, J. F. & ARBOGAST, C. L. (1960). *J. Appl. Phys.* **31**, 99–102.

STEVENS, E. D. & COPPENS, P. (1975). *Acta Cryst.* **A31**, 612–619.

STEWART, R. F. (1977). *Acta Cryst.* **A33**, 33–38.

SUORTTI, P. (1982). *Acta Cryst.* **A38**, 648–656.

WEISS, R. J. (1978). *Philos. Mag.* **B37**, 659–662.

WHITESIDE, R. A., KRISHNAN, R., POPLE, J. A., KROGH-JESPERSEN, M., SCHLEYER, P. v. R. & WENKE, G. (1980). *J. Comput. Chem.* **1**, 307–322.

WILSON, A. J. C. (1942). *Nature (London)*, **150**, 151–152.

YANG, Y. W. & COPPENS, P. (1978). *Acta Cryst.* A **34**, 61–65.